TOWARDS CIGS SOLAR CELLS WITH REDUCED FILM THICKNESS: A STUDY OF OPTICAL PROPERTIES AND OF PHOTONIC STRUCTURES FOR LIGHT TRAPPING

Lucio Claudio Andreani[1], Piotr Adam Kowalczewski[1], Camilla Irine Mura[1], Maddalena Patrini[1], Maurizio Acciarri[2], Simona Binetti[2], Adele Sassella[2], Stefano Marchionna[3]
[1]*CNISM and Department of Physics, University of Pavia, Via Bassi 6, 27100 Pavia, Italy*
[2]*CNISM and Milano-Bicocca Solar Energy Research Center (MIB-SOLAR), Department of Materials Science, University of Milano – Bicocca, via Cozzi 53, 20125 Milano, Italy*
[3]*Voltasolar s.r.l. via dell'Artigianato 8, I-22078 Turate (Como), Italy*

ABSTRACT: In view of large-scale exploitation of $CuIn_{1-x}Ga_xSe_2$ (CIGS) solar cells for photovoltaic energy conversion, it would be quite important not only to increase the conversion efficiency, but also to reduce the thickness of CIGS layer in order to decrease the use of rare and expensive elements, especially Indium. In this work we perform a full study of optical properties of CIGS solar cells grown by a hybrid sputtering/evaporation process, and use the resulting optical functions for electro-optical simulations. We then introduce a texturization of the interfaces and investigate the effects of light trapping on the conversion efficiency. Starting from a CIGS thickness around 2 μm, we show that the same or even higher efficiency can be achieved with much reduced film thickness, with a sizeable effect due to the photonic structure.

Keywords: $Cu(InGa)Se_2$, spectroscopic ellipsometry, light trapping, photonic structures

1 INTRODUCTION

$CuIn_{1-x}Ga_xSe_2$ (CIGS) solar cells are one of the most promising examples of thin film photovoltaic devices. In thin-film solar cell technology the high optical absorption of the active material is exploited in order to decrease the thickness of the active layer by a factor 10^2 relatively to crystalline- and multicrystalline-Si cells with the result of a reduction of the cost and of the energy payback time of the cell. CIGS is a quaternary I-III-VI semiconductor compound with a chalcopyrite crystalline structure and a p-type conductivity due to native defects. CIGS solar cells have the advantage of presenting a thin active layer (1 - 5 μm) thanks to the direct band gap of the material as well as efficiency and stability comparable with those of crystalline silicon cells (the actual record efficiency for CIGS solar cells is 20.3 ± 0.6 % [1]).

CIGS solar cells comprise several layers, as shown in Fig. 1 where the structure of the cells considered in this study is presented. CIGS solar cells present a Mo back contact grown on a glass, steel or polymeric substrate, a p-type CIGS active layer, an n-type CdS layer that completes the hetero-junction and a double layer of transparent conductive oxides, in our case ZnO and ITO, that forms the front contact.

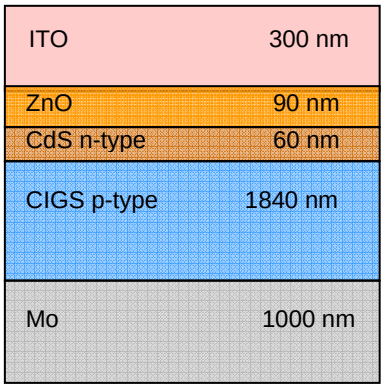

Figure 1: Schematic representation of the CIGS solar cell considered in the simulations (cell # 160).

The goal of this work is the study of the optical and electrical properties of CIGS solar cells produced with an innovative hybrid sputtering/evaporation process developed by the Milano-Bicocca Solar Energy Research Center (MIB-SOLAR) and Voltasolar srl with the aim of optimizing the performance of the cells in view of their large-scale production. Details about the deposition process are reported in Refs. [2,3].

The use of an innovative technique for the deposition of both Mo and CIGS layers justifies the need for an analysis of the optical properties of the materials, which constitutes the first part of this work. Once the optical functions of the Mo and CIGS layers of the cell under investigation are obtained, they are adopted in the electro-optical simulations of the entire structure in order to calculate its figures of merit. The electro-optical simulations are performed using Silvaco International, Inc. ATLAS software package and investigate both the case of basic cells with flat interfaces and the effects of introducing a 1D photonic structure at the CIGS/CdS or at the ITO/air interface. The variations introduced in the photovoltaic performance are studied in order to investigate the possibility of exploiting light trapping to reduce the thickness of the CIGS layer without decreasing the efficiency of the cell.

The new hybrid sequential process for CIGS solar cell production developed by Voltasolar s.r.l./MIB-SOLAR comprises several steps. The depositions are performed using a reduced dimension single vacuum chamber comprising two DC magnetron sputtering heads and an evaporation chamber [3]. The first step of CIGS solar cells production is the deposition of the Mo back contact on a glass substrate, obtained with DC magnetron sputtering technique. The sequential technique used to deposit the CIGS active layer comprises two stages, the first one is the deposition of the metallic Cu-In-Ga precursors by sequential sputtering from In targets and Cu-Ga (28 at.%) alloy targets with DC magnetron sputtering. The second step is the selenization of the metallic precursors obtained by thermal evaporation using solid pellets as Selenium sources. For the realization of the complete photovoltaic cell several other steps are required. First of all, a CdS layer is deposited by

chemical bath deposition using a solution of cadmium acetate as a source of Cd, thiourea as a source of S, ammonium chloride and ammonia. Then the ZnO and ITO layers are grown with RF sputtering and the metal top contacts are deposited by evaporation.

2 DETERMINATION OF OPTICAL FUNCTIONS

The optical characterization is carried out on Mo samples and on CIGS samples with varying composition provided by Voltasolar s.r.l./MIB-SOLAR by means of Spectroscopic Ellipsometry (SE) and is complemented by Scanning Electron Microscopy (SEM) imaging of the sample surfaces, see Fig. 2(b) and (c). SE measurements are conducted with a J. A. Woollam Co., Inc. variable angle spectroscopic ellipsometer (VASE®) using a scan in the 0.3 - 1.65 μm wavelength range with a 5 nm-step and angles of incidence 65°, 70° and 75°. SE data are analyzed using WVASE32® dedicated software in order to obtain the optical functions of CIGS and Mo by means of a best-fit procedure that adopts a multilayer model for the samples.

The optical characterization of Mo samples evidences a structural anisotropy in the response due to the ordered elongated structures observed in the SEM images of the samples. Namely, the optical response depends on the orientation of the plane of incidence relatively to the direction of the elongated structures. Nonetheless, in the case of plane of incidence parallel to the orientation of Mo surface structures the optical functions obtained experimentally are consisted with those reported in the literature [4].

A dependence of the optical response of the samples on the surface morphology is evidenced also for CIGS. Figure 2(a,b) shows a comparison between the optical functions obtained for three of our samples (# 155, # 160 and # 174) and those reported by Paulson et al. [5] for a CIGS sample with analogous composition deposited with co-evaporation and that presents a smooth surface. The spectral features of our optical functions are consistent with those reported in the literature, but there is a general reduction in the index of refraction and a different behavior of the extinction coefficient that can be due to both the different deposition method and to the surface morphology of our samples. The latter explanation is supported by the fact that samples with particularly anomalous surface structure, for example # 174 (see Fig. 2(c,d), present even lower optical functions. Despite all the factors that impact the optical properties of our CIGS samples a general characteristic is found in terms of a high absorption coefficient.

The generalized oscillator model described by Eq. 1 is adopted to reproduce the complex dielectric function of the CIGS samples and to study the dependence of the critical points on the composition of the material:

$$\boldsymbol{\varepsilon}(E) = \boldsymbol{\varepsilon}_{\infty} + 3\ \mathrm{CPPB}(E) + 6\ \mathrm{LOR}(E) \qquad (1)$$

where $\boldsymbol{\varepsilon}_{\infty}$ is the value of the dielectric function at high energies. Here the three fundamental gap transitions are accounted for with critical point parabolic band oscillators (CPPB) while the other features of the dielectric function are reproduced using six Lorentzian lineshapes (LOR). The analysis of the dielectric functions

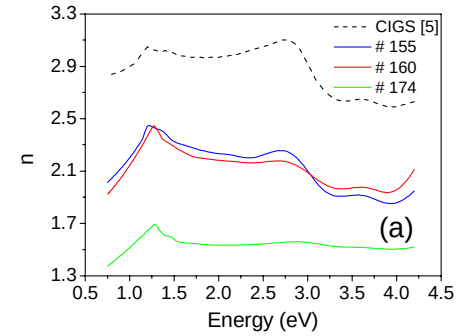

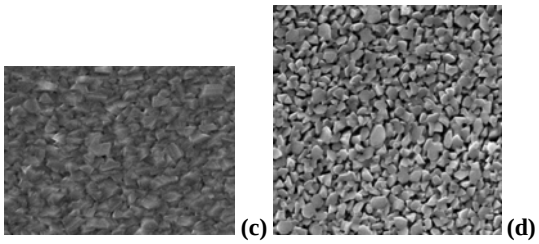

Figure 2: CIGS optical functions compared with literature [5] **(a,b)**. SEM images of samples # 160 **(c)** and # 174 **(d)**.

of the CIGS samples provides an insight in the relationship between the energies of interband critical points and the Ga and Cu content, indicated by *x* and *M* respectively, where *x* = Ga/(Ga+In) and *M* = Cu/(Ga+In). These dependences are shown in Fig. 3 for the fundamental gap transition $E_0(A)$, analogous relationships are found for higher energy transitions. According to the theory and to experimental data reported by several studies [5, 6], the fundamental band gap should increase with the Ga content x following the equation:

$$E_G(x) = E_G(0) + ax + bx^2. \qquad (2)$$

The data obtained for our samples do not confirm the expected relationship, in fact, the fundamental band gap tends to decrease as *x* grows. This behavior is related to the fact that for our samples the variation in *M* is much larger than that in *x*. For this reason our data are consistent with the theoretically expected decrease of $E_0(A)$ with the increase of *M*, as it is clear from Fig. 3(a), nonetheless, for our samples the expected dependences of the transition energies on Ga and Cu contents combine in such a way that it is not possible to completely isolate the effects due to the variation in the content of single species. In order to keep into account the effects of both Ga and Cu variations in CIGS composition we define a

new parameter z = (x+1-M)/2, where z = 0 corresponds to ideal CIS (x = 0, M = 1), and z = 1 to an hypothetical GS sample (x=1, M=0), i.e. a CGS without Cu. Fig. 3(b) presents a plot of the dependence of $E_0(A)$ on z, which is such that an increase in z is related to an increase in the transition energy.

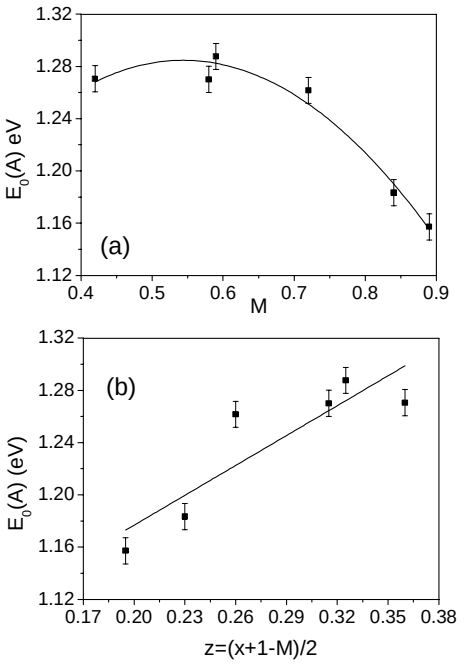

Figure 3: Dependence of CIGS fundamental gap transition on Cu **(a)** and both Ga and Cu **(b)** contents.

3 PV PERFORMANCE SIMULATIONS

The optical functions obtained for Mo and CIGS are used as numerical inputs for the electro-optical simulations of CIGS solar cells performed using the Silvaco International, Inc. ATLAS software. The JV characteristics and the internal and external quantum efficiencies (IQE and EQE) of the cells are extracted by Silvaco ATLAS after the calculation of the photogeneration profile. All the simulations are performed considering as reference the cell in which CIGS from sample # 160 is used for the active layer. This reference device is indicated as cell # 160, the thickness values of its layers are reported in Fig. 1. The electrical parameters of the simulation are either measured or adjusted in order to reproduce the experimental figures of merit of the reference cell (J_{sc} = 27.3 mA/cm^2, V_{oc} = 436.77 mV, FF = 58.4%, η =6.98%). A good agreement with the experimental results is found considering Shockley-Read-Hall (SRH) and surface recombination (SR), the values of the parameters adopted in the simulations are reported in Table I.

We now introduce one-dimensional photonic lattices for light trapping in the solar cell structure [9,10]. The results of finite-difference time domain (FDTD) simulations for the optical absorption are shown in Fig. 4. It is clear from these results that patterning of the CIGS layer has basically no effect, while patterning of ITO considerably increases the absorption. The reason is that patterning of ITO strongly reduces Fabry-Pérot oscillations arising from interference in the two oxide layers (ITO and ZnO) through better impedance matching

Layer	Parameter	Value	Unit
Mo	Sheet Resistance	1 [7]	Ω/□
CIGS	Acceptor Density	2 10^{16}	cm^{-3}
CIGS	SRH Rec Time	0.25	ns
CIGS	e Mobility	20 [8]	cm^2/Vs
CIGS	h Mobility	2.5 [8]	cm^2/Vs
CdS/CIGS	SR Velocity	10^5	cm/s
CdS	Donor Density	5 10^{16}	cm^{-3}
CdS	e Mobility	100 [8]	cm^2/Vs
CdS	h Mobility	25 [8]	cm^2/Vs
ZnO	Resistivity	1.5 10^4	μΩ cm
ITO	Sheet Resistance	120	Ω/□

Table I: Values of the parameters used in the simulations of cell # 160, the values in red were varied in order to reproduce the experimental figures of merit.

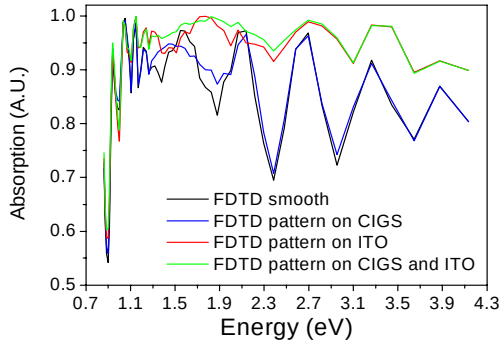

Figure 4: Simulated optical absorption for the unpatterned (smooth) cell and for patterning of CIGS, ITO, or both.

at the air/ITO interface. In other words, the patterned ITO layer acts as an anti-reflection coating at the cell surface. The parameters of the chosen 1D patterning are indicated in the structure of Fig. 5, which is considered in the rest of this Section.

The calculated J-V characteristics for the smooth and patterned solar cell structure are shown in Fig. 6. The main effect of patterning is to increase the short-circuit current, while the open-circuit voltage is nearly unaffected. The increase of J_{sc} is due to improved anti-reflection properties of the oxide layers, as discussed above.

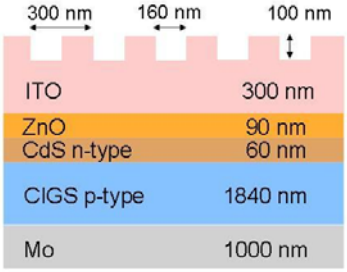

Figure 5: Structure of cell #160 with patterned ITO layer.

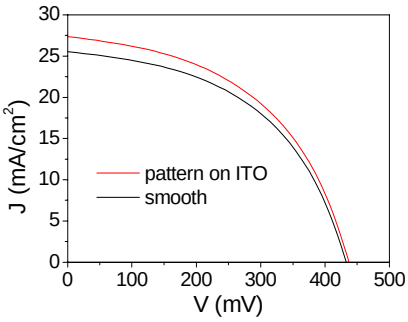

Figure 6: Simulated J-V characteristics for cell # 160, unpatterned and with patterned ITO layer.

Finally, in Fig. 7 we show the figures of merit of the solar cells as a function of CIGS thickness, for both unpatterned and patterned structures. The short-circuit current is seen to have a maximum around 1 μm thickness. The open-circuit voltage has minor variations (except for very small thickness, below 200 nm) and the fill factor has a slightly irregular behavior but without strong variations. The results energy conversion efficiency has also a maximum at a CIGS thickness around 1 μm, but even at 200 nm CIGS thickness it is larger than for the actual solar cell (CIGS thickness = 1.84 μm). The improvement due to patterning of the ITO layer is appreciable and it is nearly constant (in absolute efficiency increase) as the CIGS thickness is varied.

It should be remarked that the low absolute values of the efficiency are not relevant, as they are obtained on samples that were grown just after a technological upgrade of the sputtering/evaporation equipment. CIGS solar cells produced at Voltasolar s.r.l./MIB-SOLAR solar now reach efficiencies in the 12%-14% range routinely. A similar behavior as a function of CIGS thickness, and upon patterning of the ITO layer, is expected for these samples. Analysis of current samples by the same methodology shown in the present work is in progress.

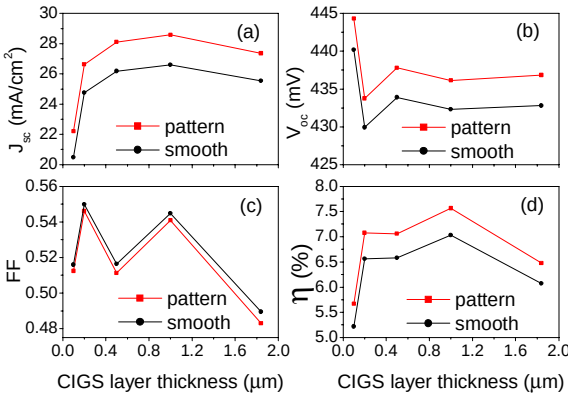

Figure 7: Short-circuit current, open-circuit voltage, fill factor, and conversion efficiency as a function of CIGS thickness, with unpatterned and with patterned ITO layer. Apart from CIGS thickness, parameters of cell # 160 are adopted.

4 CONCLUSIONS

The optical functions of Mo and CIGS layers for solar cells produced by a hybrid sputtering/evaporation process have been determined by spectroscopic ellipsometry. The optical functions obtained experimentally show spectral features similar to those reported in the literature, even though the surface morphology of the samples strongly influences the results. The critical point analysis evidenced the relation between interband transition energies and CIGS composition: an increase in the Ga content or a decrease in the Cu content cause the energy of the transitions to increase.

These optical functions, together with measured electrical parameters, have been taken as inputs for electro-optical simulations and for studying the effect of photonic structures. Patterning the ITO layer improves the conversion efficiency through better anti-reflection action. The optimal CIGS thickness is calculated to be around 1 μm, and the thickness can be reduced down to a few hundreds of nm without substantial loss of efficiency.

Acknowledgements - This work was supported by the EU through Marie Curie Action FP7-PEOPLE-2010-ITN project no. 264687 ”PROPHET”, and by Fondazione Cariplo under project 2010-0523 ”Nanophotonics for thin-film photovoltaics”.

5 REFERENCES

[1] M. A. Green et al., Prog. Photovolt.: Res. Appl. 19, (2011) 565.
[2] M. Acciarri, A. Le Donne, M. Morgano, L. Caccamo, L. Miglio S.Marchionna, R. Moneta, M. Meschia and S.Binetti, Energy Procedia 10 (2011) 138 – 143.
[3] M. Acciarri, S. Binetti, A. Le Donne, B. Lorenzi, L. Caccamo, L. Miglio, R. Moneta, S. Marchionna, M. Meschia, Cryst. Res. Technol. 46 (2011) 871.
[4] D. W. Lynch, W. R. Hunter, *Optical Constants of Metals* edited by E. D. Palik in *Handbook of Optical Constants of Solids*, Academic Press Inc. (1998).
[5] P. D. Paulson, R. W. Birkmire W. N. Shafarman, J. Appl. Phys. 94**,** No 2 (2003) 879.
[6] M. I. Alonso, K. Wakita, J. Pascual, M. Garriga, N. Yamamoto, Phys. Rev. B 63 (2001) 075203.
[7] A.M. Hermanna, C. Gonzalez, P.A. Ramakrishnan, D. Balzar, N. Popa, P. Rice, C.H. Marshall, J.N. Hilfiker, T. Tiwald, P.J. Sebastian, M.E. Calixto, and R.N. Bhattacharya., Solar Energy Materials & Solar Cells 70 (2001) 345.
[8] J. Krc, G. Cernivec, A. Campa, J. Malmström, M. Edoff, F. Smole and M. Topic, Optical and Quantum Electronics 38 (2006) 1115.
[9] A. Bozzola, M. Liscidini, L. C. Andreani, Optics Express Vol. 20, No. S2 (2012) A224.
[10] L.C. Andreani, A. Bozzola, P. Kowalczewski, M. Liscidini, Proceedings of 27th PVSEC (this conference), paper no. 1CV.8.27.